

Fully-Featured Attribute Transfer

De Xie¹, Muli Yang¹, Cheng Deng^{1,*}, Wei Liu², Dacheng Tao³

¹School of Electronic Engineering, Xidian University, Xi'an 710071, China

²Tencent AI Lab, Shenzhen, China

³UBTECH Sydney AI Centre, SIT, FEIT, University of Sydney, Australia

{xiede.xd, muliyang.xd, chdeng.xd}@gmail.com, wliu@ee.columbia.edu, dacheng.tao@sydney.edu.au

Abstract

Image attribute transfer aims to change an input image to a target one with expected attributes, which has received significant attention in recent years. However, most of the existing methods lack the ability to de-correlate the target attributes and irrelevant information, i.e., the other attributes and background information, thus often suffering from blurs and artifacts. To address these issues, we propose a novel Attribute Manifold Encoding GAN (AME-GAN) for fully-featured attribute transfer, which can modify and adjust every detail in the images. Specifically, our method divides the input image into image attribute part and image background part on manifolds, which are controlled by attribute latent variables and background latent variables respectively. Through enforcing attribute latent variables to Gaussian distributions and background latent variables to uniform distributions respectively, the attribute transfer procedure becomes controllable and image generation is more photo-realistic. Furthermore, we adopt a conditional multi-scale discriminator to render accurate and high-quality target attribute images. Experimental results on three popular datasets demonstrate the superiority of our proposed method in both performances of the attribute transfer and image generation quality.

1. Introduction

The task of image attribute transfer aims at manipulating a source image to possess single or multiple target attributes (e.g., eyeglasses, bangs, and mustaches of facial images. See Fig. 1). The desired results should not only contain the attributes of interest, but also keep other attributes and background invariant, such as the identity of a facial image. Early attempts [5, 6, 31, 36] often address this problem in a regression fashion by explicitly designing the loss functions, such as pixel-wise losses, and the target attribute is thereby learned by inputting a pair of images that only dif-

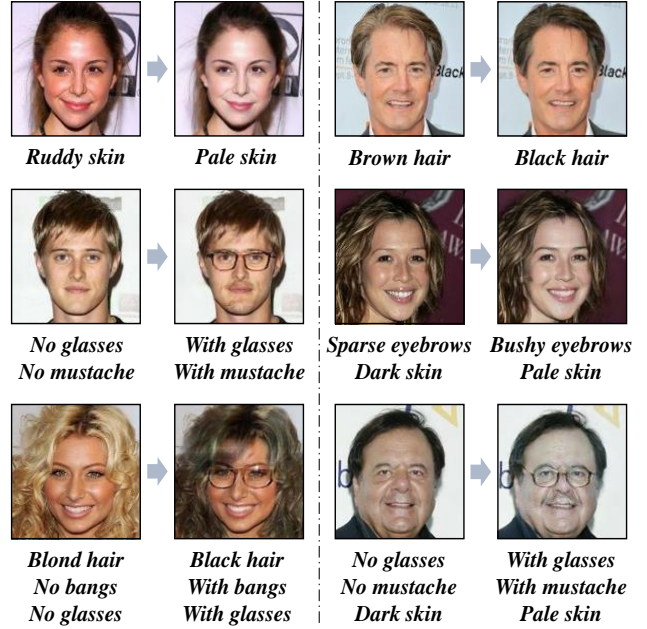


Figure 1. The illustration of our attribute transfer results for facial images, which contain single-attribute transfer and multiple-attribute transfer.

fer from the desired attribute (e.g., facial images of the same person with or without eyeglasses). Although such methods can precisely capture the target attributes from paired images, the paired images are actually difficult to attain and are thus unaffordable in real-world applications.

With the success of Generative Adversarial Networks (GANs) [7] in diverse computer vision tasks [2, 13, 12, 32, 28, 3, 33], GAN based methods [35, 34, 25, 26, 4, 27] are springing up and have exhibited promising performance on image attribute transfer. By implicitly defining the loss function with a discriminator network which is trained in an adversarial manner with the generator network, GAN based methods are more flexible in the unpaired training scenario. CycleGAN [35] harnesses a cycle structure to perform attribute transfer as a cross-domain image-to-image translation task, which is able to transfer a single attribute from

*Corresponding author

a source image to the target one. GeneGAN [34] learns an attribute subspace by encoding an input image into an attribute-relevant part and an attribute-irrelevant part, which can transfer a single attribute through toggling the two encoding parts in the learned subspace. However, these methods are only able to transfer a single attribute at a time, which are inflexible for the multiple-attribute scenario.

For multiple-attribute transfer, some recent studies [11, 25, 26, 27] argue that multiple attributes of an image can be disentangled into different parts in a latent encoding space. However, these methods have a limited capability to separate the attributes and background in the latent encoding space, which renders mutual interference during attribute transfer and often bring blurs and artifacts in the generated images. StarGAN [4] designs a multi-domain cycle structure and carries out multiple-attribute transfer by inputting an image and its corresponding binary attribute label. However, it simply regards attribute transfer as a multi-domain image-to-image translation task, which lacks the ability to model attributes effectively and cannot disentangle multiple attributes, thereby failing to control the procedure of attribute transfer.

In this paper, we propose an *Attribute Manifold Encoding GAN* (AME-GAN) to realize fully-featured attribute transfer. One can regard an image with attributes naturally lies on a high-dimensional manifold \mathcal{M}_I , which can be further divided into two submanifolds for the attributes and background separation based on the nonlinear separability of manifold. On the basis of this observation, we elaborately devise an attribute decoder and a background decoder to project attribute latent variables and background latent variables to the two submanifolds, *i.e.*, \mathcal{M}_A and \mathcal{M}_B , which can effectively separate attributes and background information. Specifically, i.i.d. Gaussian distributions and uniform distributions are respectively imposed on attribute latent variables and background ones to describe the independence of different attributes and the consistency of background information. In this way, we can modify and adjust every detail in the images with realistic generated results through recombining the target attributes information and the background information on manifold. To ensure the accuracy and high-resolution of transferred images, we design a conditional multi-scale discriminator to classify attributes and distinguish images from different scales.

Our contributions can be summarized in four-fold:

- As we know, we address the multiple-attribute transfer task via manifold learning for the first time, and separate image attributes and background information based on the nonlinear separability of manifold.
- We devise a novel framework for fully-featured attribute transfer. Especially, we design a conditional multi-scale discriminator to generate accurate and high-resolution transferred images.

- We employ Gaussian and uniform distributions to describe the independence of different attributes and the consistency of background information, respectively, which can not only preserve background information but also transfer attributes flexibly and realistically.
- Comprehensive experimental results demonstrate the superiority of our method in both the accuracy of attribute transfer and the quality of image generation under various scenarios.

2. Related Work

2.1. Image Attribute Transfer

Recently, numerous image attribute transfer methods have been proposed, which can be mainly divided into two types: optimization-based methods and learning-based methods. The main idea of optimization-based methods, such as CNAI [14] and DFI [23], is to find the difference between an input image and the target one with desired attributes, and then design a loss function to model the difference between them. In contrast, learning-based methods have received increasing attention in recent years due to their flexibility and expandability. Variational Autoencoder (VAE) and Generative Adversarial Network (GAN) based methods [7, 10, 15] are designed to learn an attribute latent representation and a corresponding decoder, which can realize attribute transfer through modifying the latent representation of input images to be close to that of the target images, followed by the decoder. IcGAN [20] combines cGAN [19] with an encoder. It can sample from a uniform distribution to obtain the latent representation irrelevant to input image attributes, and then encode the target attributes into this latent representation and decode it to obtain the image with target attributes. Some image translation methods, such as CycleGAN [35], are able to transfer images across image domains.

Other attempts explore exchanging latent codes in the latent attribute space of the input images to implement attribute transfer. GeneGAN [34] swaps a specific attribute between two given images by recombining the information of their latent representations. TD-GAN [25] and DNA-GAN [26] also exchange attribute latent code blocks between a given pair of images to generate hybrid images. ELEGANT [27] applies a U-Net structure [22] on the basis of DNA-GAN for high-resolution image generation. StarGAN [4] and AttGAN [8] realize attribute transfer by introducing an attribute classification loss. Moreover, StarGAN [4] designs a conditional attribute transfer network to learn attributes in a cyclic process, while AttGAN [8] devises an encoder-decoder architecture to model the relationship between the latent representations and the attributes. Both StarGAN and AttGAN are designed for learning multiple attributes simultaneously. However, they fail to frame

attribute information sufficiently by only concatenating attribute labels to image latent variables, which is limited to decoupling the correlation of different attributes and leads to unrealistic results.

Our proposed method can cope with both image attributes and background information by mapping images to a latent space and encode them to the corresponding latent representations. The independence of different attributes and the consistency of background information are respectively preserved through imposing Gaussian and uniform distributions on the latent representations. These latent representations are then projected to the manifolds conditional on the target attributes through two deconvolutional generators to handle the attributes and the background information separately and flexibly. This scheme can make the procedure of attribute transfer more explicable and provide an effective solution to all the problems mentioned above.

2.2. Generative Adversarial Network

Generative Adversarial Network (GAN) has been widely used for image generation tasks [1, 17, 18, 29]. GAN comprises two components: a generator G and a discriminator D . The generator G captures the distribution of training samples and learns to generate new samples imitating the training ones, and the discriminator D tries to distinguish the generated samples from the training ones. G and D are trained adversarially with each other using a *min-max game* strategy. The objective function of GAN is given as follows:

$$\min_G \max_D \mathbb{E}_{x \sim p_{data}(x)} [\log D(x)] + \mathbb{E}_{z \sim p_z(z)} [\log(1 - D(G(z)))], \quad (1)$$

where z denotes a vector randomly sampled from a prior distribution $p_z(z)$, and $p_{data}(x)$ is the data distribution. There are many variations of GAN. DCGAN [21] adopts deconvolutional and convolutional neural networks to implement G and D , respectively, which promotes the application of GANs in many image generation tasks. cGAN [19] modifies GAN from unsupervised learning to semi-supervised learning by feeding the conditional variables into the data and achieves promising performance.

In this paper, we design a conditional multi-scale discriminator. Through introducing multi-scale conditional discriminative information to the discriminator, we can significantly improve the performance of GANs and therefore generate accurate images with high quality.

3. Attribute Manifold Encoding GAN

3.1. Overview

In the attribute transfer task, an image with attributes can be divided into two components: the attribute part and the background part. The background part should remain unchanged while flexibly changing the attribute part. Sup-

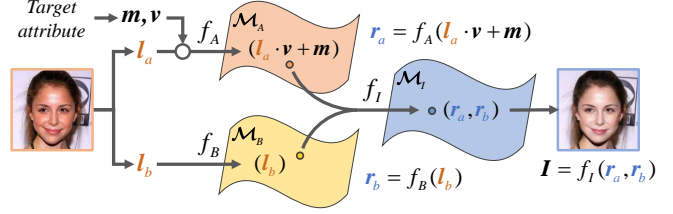


Figure 2. The pipeline of the proposed approach.

pose that an image I with multiple attributes lies on a high-dimensional manifold \mathcal{M}_I , on which traversing along a certain direction could achieve attribute transfer while preserving the image background information. Mathematically, the mapping process can be formulated as follows:

$$I = f_I(r_a, r_b), \quad (2)$$

where r_a and r_b are the representations of image attributes and background, respectively. f_I is the mapping from r_a and r_b to \mathcal{M}_I . In order to customize attributes, we assume r_a lies on a submanifold of \mathcal{M}_I , denoted by \mathcal{M}_A , which can be controlled with the attribute label x and the attribute latent variable l_a . It can be formulated as:

$$r_a = f_A(l_a, x), \quad (3)$$

where f_A is the mapping from l_a and x to \mathcal{M}_A . For the fully-featured attribute transfer, the different attributes should be independently identically distributed. According to Variational Autoencoder (VAE) [10], we impose i.i.d. Gaussian distributions on the attribute latent variable l_a and apply different means m_x and variances v_x generated from the target attribute label x to represent different attributes. Thus, Eq. (3) can be rewritten as follows:

$$r_a = f_A(l_a \cdot v_x + m_x). \quad (4)$$

By doing so, the independence and heterogeneity of different attributes can be described by i.i.d. Gaussian distributions and their means and variances, which is efficient and reasonable for fully-featured attribute transfer.

Regarding the background part representation, r_b can be assumed to lie on another submanifold of \mathcal{M}_I , denoted by \mathcal{M}_B , and is controlled by the background latent variable l_b , which can be denoted as:

$$r_b = f_B(l_b), \quad (5)$$

where f_B is the mapping from l_b to \mathcal{M}_B . In order to keep the consistency of background information, inspired by CAAE [32], we take advantage of the uniformity of a uniform distribution and impose it on the background latent variable l_b , which can render the background information smooth on \mathcal{M}_B and thus generate undistorted images. Fig. 2 illustrates the pipeline of the proposed approach.

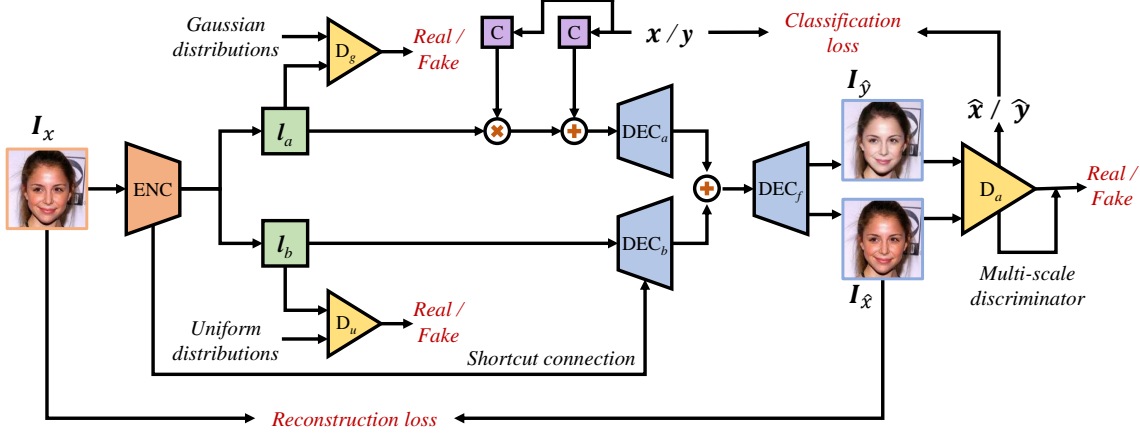


Figure 3. The flowchart of the proposed framework, which comprises three main components, *i.e.*, Encoder, Decoder, and Discriminator. Given an image as input, Encoder generates two latent variables l_a and l_b for the attribute part and the background part respectively. Decoder modifies l_a by the target attribute label, which is then coupled with l_b for synthesizing an image with target attributes on manifolds. Discriminator imposes Gaussian and uniform distributions on l_a and l_b respectively, and moreover, encourages the generated image to be photo-realistic and reliable towards target attributes.

3.2. Framework

We propose a novel framework for fully-featured attribute transfer using manifold learning. The whole architecture is illustrated in Fig. 3. It contains three blocks: 1) an image encoder block ENC that encodes an image to the attribute latent variable l_a and the background latent variable l_b ; 2) a decoder block, including three parts: an attribute decoder DEC_a , a background decoder DEC_b , and a fusion decoder DEC_f , which map (l_a, x) to \mathcal{M}_A , l_b to \mathcal{M}_B , and (r_a, r_b) to \mathcal{M}_I , respectively; 3) a discriminator block, including three parts: a Gaussian discriminator D_g , a uniform discriminator D_u and an attribute discriminator D_a . D_g and D_u regularize l_a to Gaussian distributions, and l_b to uniform distributions, respectively. D_a is a conditional multi-scale discriminator, which ensures attribute transferred images more accurate and of higher resolution through attribute classification and multi-scale image information discrimination.

Encoder. Given an image I_x with n binary attributes $x = (x_1, x_2, \dots, x_n)$ and target attributes $y = (y_1, y_2, \dots, y_n)$, we can obtain the attribute latent variable l_a and the background latent variable l_b , which can be written as:

$$(l_a, l_b) = \text{ENC}(I_x). \quad (6)$$

Decoder. In order to map (y, l_a) to \mathcal{M}_A and l_b to \mathcal{M}_B , we design the image attribute decoder DEC_a and the image background decoder DEC_b , which are expected to learn f_A and f_B , respectively. For DEC_a , firstly, two extra groups of convolutional layers are designed to learn the mean m_y and variance v_y of target attributes. The attribute representation r_a^y , which lies on the submanifold \mathcal{M}_A , can be formulated as:

$$r_a^y = \text{DEC}_a(\theta \cdot (l_a \cdot v_y + m_y)), \quad (7)$$

where θ is a hyper-parameter (set to 1.0 during training) that can control the intensity of attribute transfer. For DEC_b , the background representation r_b , which lies on the submanifold \mathcal{M}_B , can be depicted as:

$$r_b = \text{DEC}_b(l_b). \quad (8)$$

After obtaining r_a^y and r_b , DEC_f is designed to combine them and map them to \mathcal{M}_I to generate an attribute transferred image, which can be denoted as:

$$I_y = \text{DEC}_f(r_a^y + r_b). \quad (9)$$

We introduce a reconstruction loss to measure the correctness of attribute learning, which ensures that the information of attributes is preserved in r_a^y . The reconstruction loss can be written as:

$$\mathcal{L}_{recon} = \mathbb{E}_{y=x} [\|I_y - I_x\|_1]. \quad (10)$$

Discriminator. The Gaussian discriminator D_g and the uniform discriminator D_u aim to force l_a to approach Gaussian distributions and l_b uniform distributions, respectively. Suppose that g obeys a set of Gaussian distributions ($g \sim N(0, 1)$) and z obeys a set of uniform distributions ($z \sim U(-1, 1)$). The objective functions of D_g and D_u can be formulated as:

$$\mathcal{L}_{adv}^g = \mathbb{E}_{g \sim N} [\log D(g)] + \mathbb{E}_{l_a \sim p(l_a)} [\log(1 - D(l_a))], \quad (11)$$

$$\mathcal{L}_{adv}^u = \mathbb{E}_{z \sim U} [\log D(z)] + \mathbb{E}_{l_b \sim p(l_b)} [\log(1 - D(l_b))]. \quad (12)$$

For the attribute discriminator D_a , we adopt a conditional multi-scale discriminator architecture to deal with the two tasks, *i.e.*, generated images discrimination and

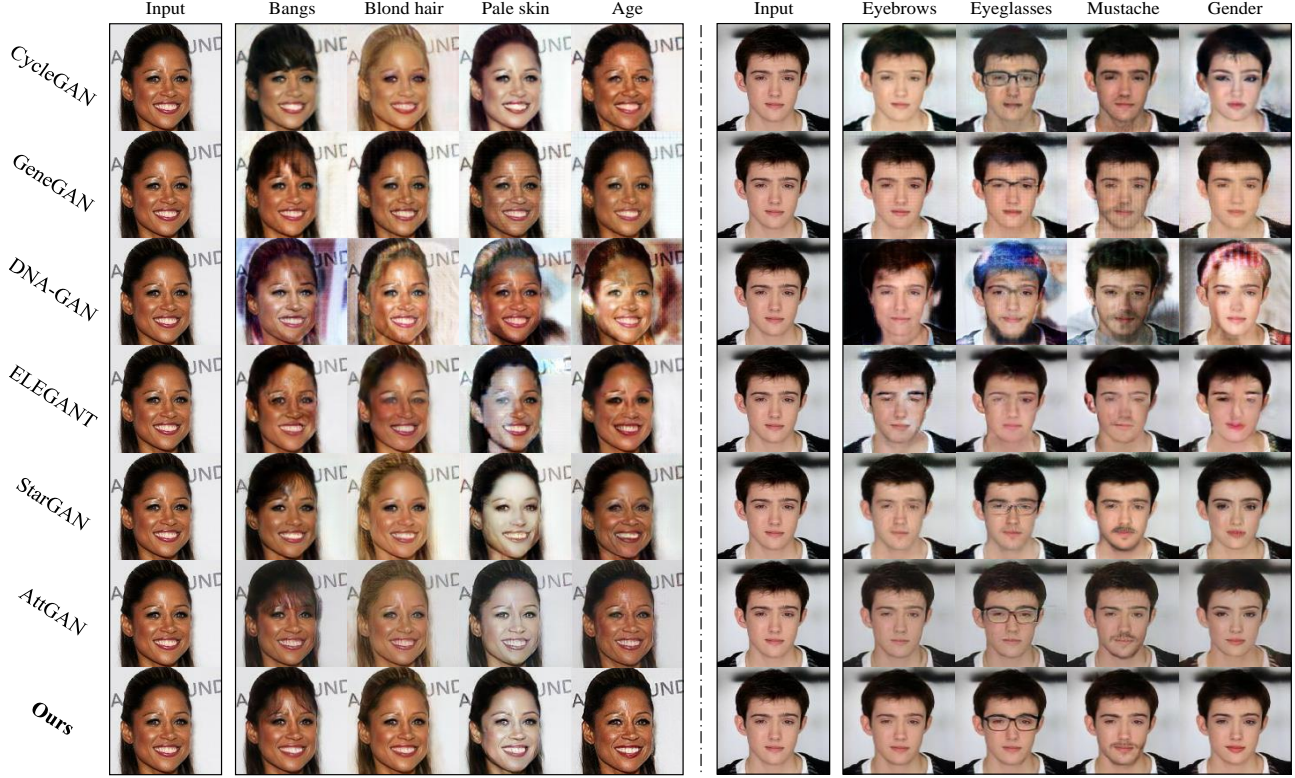


Figure 4. Single-attribute transfer results on the CelebA dataset.

attribute classification. For the first task, suppose that $\{d_1^I, d_2^I, \dots, d_m^I\}$ are the output of m different layers of D_a with I as input. The multi-scale objective function of D_a can be framed as:

$$\mathcal{L}_{adv}^a = \mathbb{E}_{I_x \sim p(I_x)} [\log \sum_{i=1}^m \gamma_i d_i^{I_x}] + \mathbb{E}_{I_y \sim p(I_y)} [\log (1 - \sum_{i=1}^m \gamma_i d_i^{I_y})], \quad (13)$$

where γ_i is the weight of multi-scale information $d_i^{I^*}$. For the attribute classification task, we adopt binary cross entropy loss to ensure efficient attribute learning. Suppose that $c = (c_1, c_2, \dots, c_n)$ is the predicted attribute label. The attribute classification objective function of D_a can be written as:

$$\mathcal{L}_{cls}^a = \sum_{i=1}^n -y_i \log c_i - (1 - y_i) \log (1 - c_i). \quad (14)$$

Combining \mathcal{L}_{adv}^a with \mathcal{L}_{cls}^a , we can obtain the overall objective function of the attribute discriminator D_a .

3.3. Objective Function

The final objective function of our method can be obtained by combining Eq. (10), Eq. (11), Eq. (12), Eq. (13), and Eq. (14):

$$\mathcal{L}_{all} = \mathcal{L}_{recon} + \mathcal{L}_{adv}^g + \mathcal{L}_{adv}^u + \mathcal{L}_{adv}^a + \mathcal{L}_{cls}^a. \quad (15)$$

The encoder, decoder and discriminator blocks are trained alternately by minimizing \mathcal{L}_{all} until convergence.

3.4. Extension to Controllable Attribute Transfer

After the training procedure, we can customize attribute transfer with the trained encoder and decoder. Given an image I_u with attributes u and the target attributes v , firstly, the image attribute latent variable l_a and the background latent variable l_b can be obtained according to Eq. (6), and eventually the transferred image I_v with the target attributes v can be achieved by:

$$I_v = \text{DEC}_f (\text{DEC}_a (\theta \cdot (l_a \cdot v_v + m_v)) + \text{DEC}_b(l_b)), \quad (16)$$

where v_v and m_v are the variances and means of the target attributes generated by the binary label of v . In addition, the intensity of attribute transfer can be controlled by the value of hyper-parameter θ .

4. Experiments

4.1. Datasets and Implementations

Datasets. We evaluate our method on three datasets: CelebA [16], Caltech-UCSD-Birds 200-2011 (CUB) [24], and Paintings dataset [35]. The CelebA dataset is composed of 202,599 facial images with 40 attributes, and 5 landmark locations. We use the aligned and cropped version and

Table 1. Single-attribute transfer accuracy on the CelebA dataset.

Method	Bangs	Blond hair	Pale skin	Age	Eyebrows	Eyeglasses	Mustache	Gender	Average
CycleGAN	0.483	0.502	0.344	0.695	0.266	0.553	0.109	0.538	0.436
GeneGAN	0.279	0.122	0.101	0.814	0.093	0.479	0.084	0.471	0.305
DNA-GAN	0.139	0.223	0.203	0.798	0.114	0.471	0.062	0.333	0.293
ELEGANT	0.397	0.313	0.232	0.858	0.166	0.337	0.092	0.479	0.359
StarGAN	0.864	0.686	0.426	0.908	0.263	0.938	0.156	0.853	0.637
AttGAN	0.513	0.638	0.651	0.895	0.367	0.962	0.278	0.967	0.659
Ours	0.825	0.585	0.713	0.944	0.458	0.978	0.328	0.975	0.726

Table 2. Perceptual similarity errors of single-attribute transfer results using LPIPS metric (v0.1) on the CelebA dataset.

Method	Bangs	Blond hair	Pale skin	Age	Eyebrows	Eyeglasses	Mustache	Gender	Average
CycleGAN	0.167	0.185	0.138	0.100	0.101	0.167	0.118	0.164	0.142
GeneGAN	0.101	0.076	0.060	0.069	0.069	0.091	0.093	0.097	0.082
DNA-GAN	0.220	0.173	0.198	0.212	0.225	0.264	0.275	0.241	0.226
ELEGANT	0.097	0.130	0.215	0.106	0.143	0.103	0.129	0.109	0.129
StarGAN	0.131	0.157	0.170	0.104	0.108	0.130	0.113	0.114	0.128
AttGAN	0.110	0.129	0.123	0.077	0.079	0.110	0.082	0.096	0.101
Ours	0.067	0.072	0.080	0.054	0.057	0.065	0.055	0.062	0.064

choose eight distinguishable attributes, *i.e.*, Bangs, Blond hair, Pale skin, Age, Eyebrows, Eyeglasses, Mustache, and Gender for all comparison methods. The CUB dataset contains 11,788 images from 200 different types of birds and 312 annotated attributes. We combine all the color attributes and select four strong visual impact attributes: Blue, Yellow, Black and Red. The Paintings dataset is collected from Flickr and WikiArt, which contains five styles, *i.e.*, Photo, Monet, Van Gogh, Cezanne and Ukiyo-e.

Implementation details. Our method is compared with the following six latest methods: CycleGAN, GeneGAN, DNA-GAN, ELEGANT, StarGAN and AttGAN, which achieve state-of-the-art performance for attribute transfer. Our propose model is trained on an NVIDIA TITAN X GPU and implemented with the TensorFlow toolkit. The encoder ENC is equipped with five layers of Conv-BatchNorm-LeakyRelu blocks, and Deconv-InstanceNorm-ReLu blocks are employed in the three decoders. Especially, we adopt the U-Net structure for DEC_b that skips connection with ENC. D_u and D_g are both equipped with two layers of 1×1 Conv-BatchNorm-LeakRelu blocks followed by a fully-connected layer. Attribute discriminator D_a uses five layers of Conv-BatchNorm-LeakRelu blocks followed by two fully-connected layers for the discriminative branch and the classification branch, respectively. All networks are trained with Adam [9] initialized with the learning rate set to 0.0002, β_1 0.5 and β_2 0.999. All the input images are normalized into the range $[-1, 1]$ and all the comparison methods are under the same experimental setting.

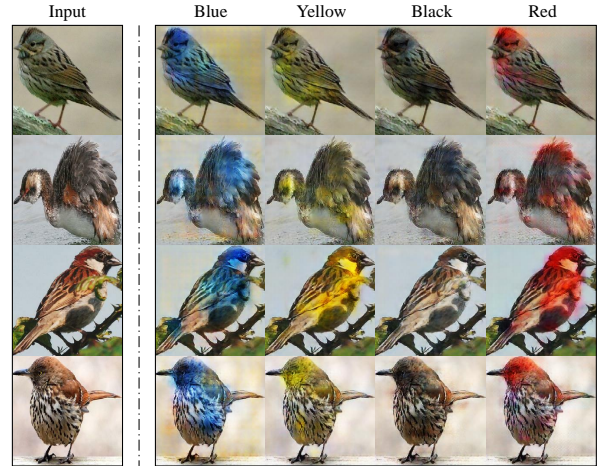


Figure 5. Single-attribute transfer results of our method on the CUB dataset.

4.2. Single-Attribute Transfer Evaluation

We first evaluate our method with CycleGAN, GeneGAN, DNA-GAN, ELEGANT, StarGAN and AttGAN on the CelebA dataset for the single-attribute transfer task. As can be seen in Fig. 4, CycleGAN is able to learn attribute information but is inefficient and generates distorted and blurred images in some cases. GeneGAN, DNA-GAN and ELEGANT require to be specified an image of target attribute to realize attribute transfer, which is susceptible to the attribute-irrelevant information of it. The results of GeneGAN, DNA-GAN and ELEGANT are often blurred and ghosted, indicating these three methods are incapable of decoupling image attributes and background effectively. For StarGAN and AttGAN, both of them can capture the

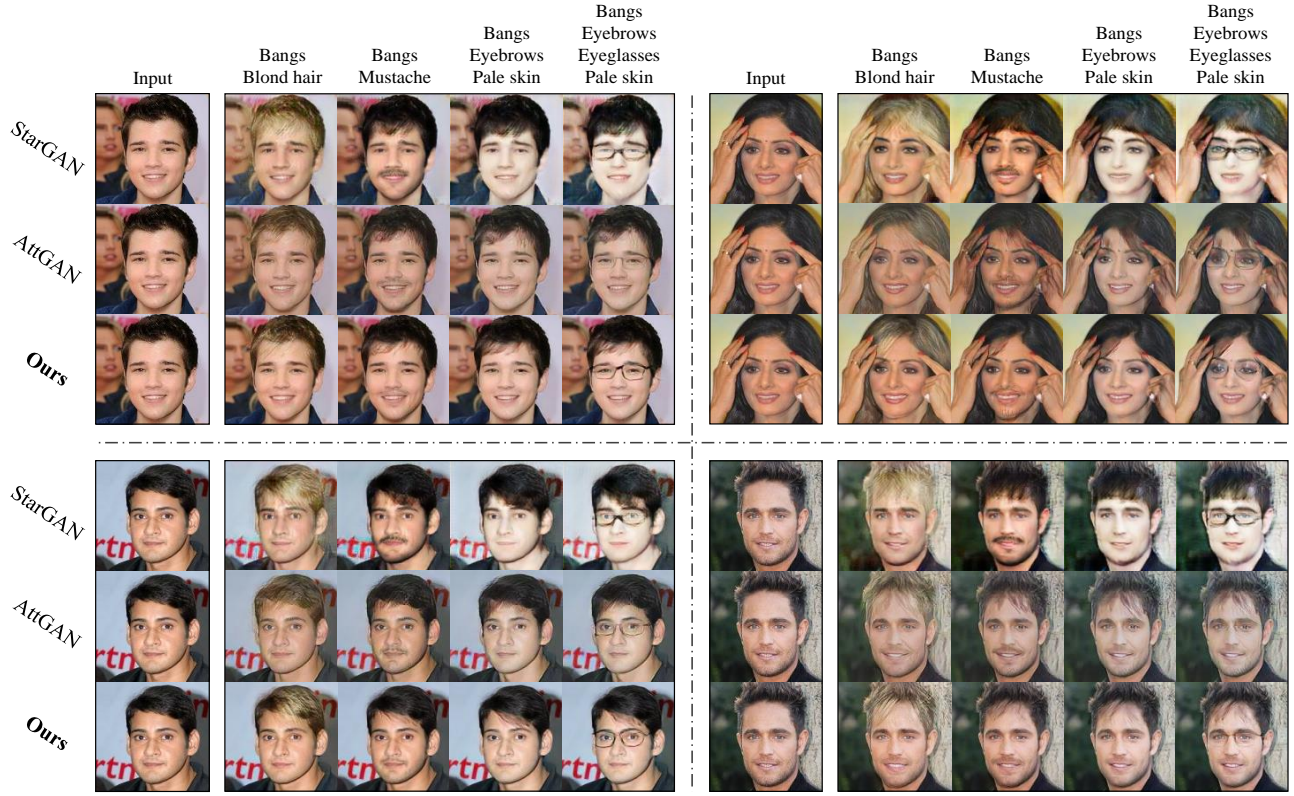


Figure 6. Multiple-attribute transfer results on the CelebA dataset.

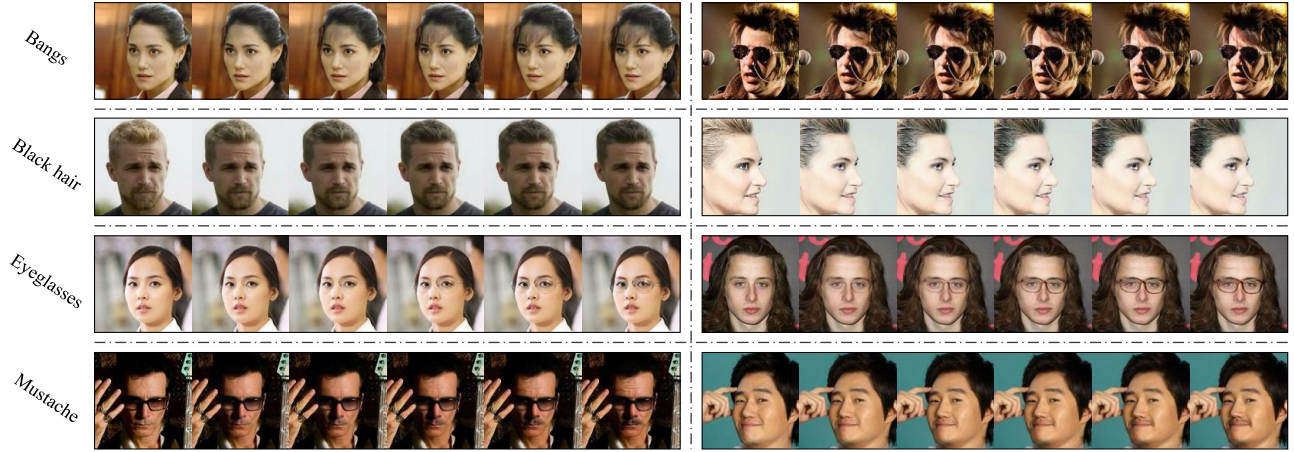


Figure 7. Controllable attribute transfer results of our method on the CelebA dataset.

attribute information accurately, but some of their results are unnatural, such as “Pale skin” and “Eyebrows”. In addition, both of their results are relatively of low-resolution. By comparison, the results of our method appear more sharp and realistic, which can fully prove that the multi-scale discriminator is conducive to generating clear images.

For quantitatively evaluate our method, we further conduct two quantitative experiments for all the methods involved. To evaluate the attribute transfer accuracy, a classifier is designed and trained on the CelebA dataset to mea-

sure the accuracy of attribute transfer of the eight attributes by judging whether a transferred image possesses the desired attribute. For evaluating the quality of attribute transferred images, we adopt the LPIPS metric [30] (v0.1) to measure the perceptual similarity error between the input images and the transferred ones, which is sensitive to blurs and artifacts, and thus the lower perceptual similarity error indicates higher-resolution and more realistic transferred images. As exhibited in Table 1 and Table 2, our method achieves the highest average attribute transfer accuracy and

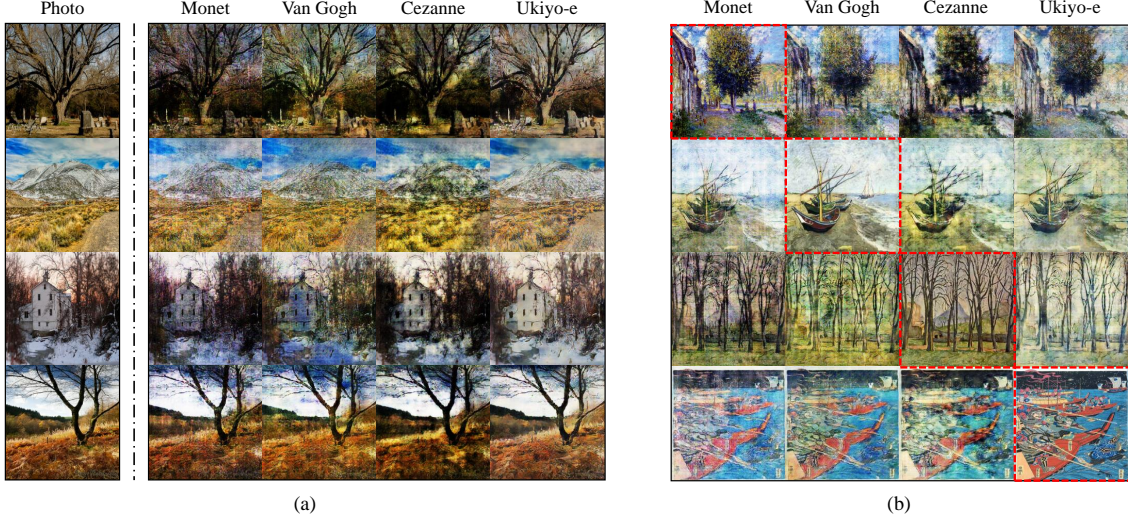


Figure 8. Photo to painting and painting to painting image translation results (respectively illustrated in (a) and (b)) of our method. Note that the red dotted frames in (b) denote input images.

the lowest average perceptual similarity error, demonstrating the ability of our method to generate accurate and realistic results.

Our method not only fits to facial attribute transfer, but can also be extended to wide range of scenarios. We conduct an experiment of feather colors transfer on the CUB dataset and obtain promising results (See Fig. 5).

4.3. Multiple-Attribute Transfer Evaluation

For multiple-attribute transfer evaluation, we conduct comprehensive experiments for StarGAN, AttGAN and our method, which can learn and transfer multiple attributes simultaneously.

As can be seen in Fig. 6, both the results of StarGAN and AttGAN are more or less distorted, such as “Pale skin” and “Eyeglasses”. Furthermore, some results are even affected by the background of images, such as “Blond hair”, and StarGAN especially suffers from artifacts. The reason of these undesired experimental results is that both StarGAN and AttGAN fail to decouple the information of different attributes effectively, which leads to true attributes can not be captured correctly. By contrast, our method can generate photo-realistic and accurate results even under complex combinations of multiple attributes. Explicitly and separately modeling image attributes and image background ensures that the attribute information and the background information are not mutually affected during generative procedure. Different attributes are described by different means and variances of attribute latent variables, which can decorrelate those highly correlated attributes effectively. Moreover, approaching background latent variables to uniform distributions ensures the generated images to be realistic. Conditional multi-scale discriminator is adopted to make the generated images accurate and high-resolution.

4.4. Controllable Attribute Transfer on Manifold

Since we adopt the idea of manifold learning for the image attribute transfer task, we can achieve a controllable and progressive transfer of attributes on the manifold. According to Eq. (7), we can control the amplitude of the attribute latent variables by controlling the value of the hyper-parameter θ , and further control the intensity of attribute transfer on the manifold. The results of controllable attribute transfer are illustrated in Fig. 7, where the range of θ is $[0, 1]$. We apply six different values for θ and obtain the corresponding progressive transferring results.

4.5. Extension to Image-to-Image Translation Task

Our method is also a general approach for the image-to-image translation task. By regarding the styles of images as attributes, we apply our method on the Paintings dataset and the results are illustrated in Fig. 8. Since image translation is a uniform transformation for both global and local information of an image while attribute transfer is only for local information, the results of Fig. 8 contain some artifacts, but can still prove that our method is a potential architecture for a wide-range of image generation tasks.

5. Conclusion

We have presented a novel AME-GAN for fully-featured attribute transfer. The attribute latent variables and background latent variables are respectively enforced to Gaussian distributions and to uniform distributions, such that every detail in the images can be modified and adjusted by these latent variables effortlessly. In order to make the attribute transferred images more accurate and realistic, we developed a conditional multi-scale discriminator to distinguish generated images, which is beneficial to yielding ac-

curate and realistic attribute transferred images. Comprehensive experimental results on three broadly used datasets demonstrate the effectiveness of the proposed approach on both attribute transfer and image translation tasks.

References

- [1] N. Bodla, G. Hua, and R. Chellappa. Semi-supervised fusedgan for conditional image generation. *arXiv preprint arXiv:1801.05551*, 2018. 3
- [2] W. Chen and J. Hays. Sketchygan: Towards diverse and realistic sketch to image synthesis. In *CVPR*, pages 9416–9425, 2018. 1
- [3] Y. Chen, Y.-K. Lai, and Y.-J. Liu. Cartoongan: Generative adversarial networks for photo cartoonization. In *CVPR*, pages 9465–9474, 2018. 1
- [4] Y. Choi, M. Choi, M. Kim, J.-W. Ha, S. Kim, and J. Choo. Stargan: Unified generative adversarial networks for multi-domain image-to-image translation. In *CVPR*, June 2018. 1, 2
- [5] L. Gatys, A. S. Ecker, and M. Bethge. Texture synthesis using convolutional neural networks. In *NIPS*, pages 262–270, 2015. 1
- [6] L. A. Gatys, A. S. Ecker, and M. Bethge. A neural algorithm of artistic style. *arXiv preprint arXiv:1508.06576*, 2015. 1
- [7] I. Goodfellow, J. Pouget-Abadie, M. Mirza, B. Xu, D. Warde-Farley, S. Ozair, A. Courville, and Y. Bengio. Generative adversarial nets. In *NIPS*, pages 2672–2680, 2014. 1, 2
- [8] Z. He, W. Zuo, M. Kan, S. Shan, and X. Chen. Arbitrary facial attribute editing: Only change what you want. *arXiv preprint arXiv:1711.10678*, 2017. 2
- [9] D. P. Kingma and J. Ba. Adam: A method for stochastic optimization. *arXiv preprint arXiv:1412.6980*, 2014. 6
- [10] D. P. Kingma and M. Welling. Auto-encoding variational bayes. *arXiv preprint arXiv:1312.6114*, 2013. 2, 3
- [11] G. Lample, N. Zeghidour, N. Usunier, A. Bordes, L. Denoyer, et al. Fader networks: Manipulating images by sliding attributes. In *NIPS*, pages 5967–5976, 2017. 2
- [12] C. Ledig, L. Theis, F. Huszár, J. Caballero, A. Cunningham, A. Acosta, A. P. Aitken, A. Tejani, J. Totz, Z. Wang, et al. Photo-realistic single image super-resolution using a generative adversarial network. In *CVPR*, page 4, 2017. 1
- [13] C. Li, C. Deng, N. Li, W. Liu, X. Gao, and D. Tao. Self-supervised adversarial hashing networks for cross-modal retrieval. In *CVPR*, June 2018. 1
- [14] M. Li, W. Zuo, and D. Zhang. Convolutional network for attribute-driven and identity-preserving human face generation. *arXiv preprint arXiv:1608.06434*, 2016. 2
- [15] M.-Y. Liu, T. Breuel, and J. Kautz. Unsupervised image-to-image translation networks. In *NIPS*, pages 700–708, 2017. 2
- [16] Z. Liu, P. Luo, X. Wang, and X. Tang. Deep learning face attributes in the wild. In *ICCV*, pages 3730–3738, 2015. 5
- [17] Y. Lu, Y.-W. Tai, and C.-K. Tang. Attribute-guided face generation using conditional cyclegan. In *ECCV*, pages 293–308. Springer, 2018. 3
- [18] S. Ma, J. Fu, C. W. Chen, and T. Mei. Da-gan: Instance-level image translation by deep attention generative adversarial networks. In *CVPR*, pages 5657–5666, 2018. 3
- [19] M. Mirza and S. Osindero. Conditional generative adversarial nets. *arXiv preprint arXiv:1411.1784*, 2014. 2, 3
- [20] G. Perarnau, J. van de Weijer, B. Raducanu, and J. M. Álvarez. Invertible conditional gans for image editing. *arXiv preprint arXiv:1611.06355*, 2016. 2
- [21] A. Radford, L. Metz, and S. Chintala. Unsupervised representation learning with deep convolutional generative adversarial networks. *arXiv preprint arXiv:1511.06434*, 2015. 3
- [22] O. Ronneberger, P. Fischer, and T. Brox. U-net: Convolutional networks for biomedical image segmentation. In *MICCAI*, pages 234–241. Springer, 2015. 2
- [23] P. Upchurch, J. R. Gardner, G. Pleiss, R. Pless, N. Snaveley, K. Bala, and K. Q. Weinberger. Deep feature interpolation for image content changes. In *CVPR*, pages 6090–6099, 2017. 2
- [24] C. Wah, S. Branson, P. Welinder, P. Perona, and S. Belongie. The caltech-ucsd birds-200-2011 dataset. 2011. 5
- [25] C. Wang, C. Wang, C. Xu, and D. Tao. Tag disentangled generative adversarial networks for object image re-rendering. In *IJCAI*, 2017. 1, 2
- [26] T. Xiao, J. Hong, and J. Ma. Dna-gan: Learning disentangled representations from multi-attribute images. *ICLR Workshop*, 2018. 1, 2
- [27] T. Xiao, J. Hong, and J. Ma. Elegant: Exchanging latent encodings with gan for transferring multiple face attributes. In *ECCV*, September 2018. 1, 2
- [28] T. Xu, P. Zhang, Q. Huang, H. Zhang, Z. Gan, X. Huang, and X. He. AttnGAN: Fine-grained text to image generation with attentional generative adversarial networks. *arXiv preprint*, 2017. 1
- [29] G. Zhang, M. Kan, S. Shan, and X. Chen. Generative adversarial network with spatial attention for face attribute editing. In *ECCV*, pages 417–432, 2018. 3
- [30] R. Zhang, P. Isola, A. A. Efros, E. Shechtman, and O. Wang. The unreasonable effectiveness of deep features as a perceptual metric. In *CVPR*, 2018. 7
- [31] Z. Zhang and Y. Peng. Eyeglasses removal from facial image based on mvlr. In *The Era of Interactive Media*, pages 101–109. Springer, 2013. 1
- [32] Z. Zhang, Y. Song, and H. Qi. Age progression/regression by conditional adversarial autoencoder. In *CVPR*, volume 2, 2017. 1, 3
- [33] B. Zhao, B. Chang, Z. Jie, and L. Sigal. Modular generative adversarial networks. *arXiv preprint arXiv:1804.03343*, 2018. 1
- [34] S. Zhou, T. Xiao, Y. Yang, D. Feng, Q. He, and W. He. GeneGAN: Learning object transfiguration and attribute subspace from unpaired data. In *BMVC*, 2017. 1, 2
- [35] J.-Y. Zhu, T. Park, P. Isola, and A. A. Efros. Unpaired image-to-image translation using cycle-consistent adversarial networks. In *ICCV*, 2017. 1, 2, 5
- [36] Z. Zhu, P. Luo, X. Wang, and X. Tang. Recover canonical-view faces in the wild with deep neural networks. *arXiv preprint arXiv:1404.3543*, 2014. 1